



## ORIGINAL ARTICLE

# Clinical and genetic characterization of *PYROXD1*-related myopathy patients from Turkey

Hülya-Sevcan Daimagüler<sup>1,2</sup>  | Ugur Akpulat<sup>1,2,3</sup> | Özkan Özdemir<sup>1,2</sup>  |  
Uluc Yis<sup>4</sup> | Serdal Güngör<sup>5</sup> | Beril Talim<sup>6</sup> | Gülden Diniz<sup>7</sup> | Figen Baydan<sup>8,9</sup> |  
Holger Thiele<sup>10</sup> | Janine Altmüller<sup>10</sup> | Peter Nürnberg<sup>2,10</sup> | Sebahattin Cirak<sup>1,2</sup>

<sup>1</sup>Department of Pediatrics, University of Cologne, Faculty of Medicine and University Hospital Cologne, Cologne, Germany

<sup>2</sup>Center for Molecular Medicine Cologne (CMMC), University of Cologne, Faculty of Medicine and University Hospital Cologne, Cologne, Germany

<sup>3</sup>Department of Medical Biology, Faculty of Medicine, Kastamonu University, Kastamonu, Turkey

<sup>4</sup>Faculty of Medicine, Department of Pediatric Neurology Izmir, Dokuz Eylül University, Izmir, Turkey

<sup>5</sup>Faculty of Medicine, Turgut Ozal Research Center, Department of Paediatric Neurology, İnönü University Malatya, Malatya, Turkey

<sup>6</sup>Pediatric Pathology Unit, Department of Pediatrics, Hacettepe University Ankara, Ankara, Turkey

<sup>7</sup>Department of Pathology, Izmir Democracy University, Izmir, Turkey

<sup>8</sup>Division of Child Neurology, Tepecik Training and Research Hospital, Izmir, Turkey

<sup>9</sup>Neuromuscular Disease Center, Tepecik Training and Research Hospital, Izmir, Turkey

<sup>10</sup>Cologne Center for Genomics (CCG), University of Cologne and University Hospital Cologne, Cologne, Germany

## Correspondence

Dr. Sebahattin Cirak, Department of Pediatrics, Faculty of Medicine and University Hospital Cologne, University Hospital Cologne, Kerpener Straße 62, 50937 Köln, Cologne, Germany.  
Email: sebahattin.cirak@uk-koeln.de

## Abstract

Congenital myopathies (CMs) are a heterogeneous group of inherited muscle disorders characterized by muscle weakness at birth, while limb-girdle muscular dystrophies (LGMD) have a later onset and slower disease progression. Thus, detailed clinical phenotyping of genetically defined disease entities are required for the full understanding of genotype–phenotype correlations. A recently defined myopathic genetic disease entity is caused by bi-allelic variants in a gene coding for pyridine nucleotide-disulfide oxidoreductase domain 1 (*PYROXD1*) with unknown substrates. Here, we present three patients from two consanguineous Turkish families with mild LGMD, facial weakness, normal CK levels, and slow progress. Genomic analyses revealed a homozygous known pathogenic missense variant (c.464A>G, p.Asn155Ser) in family 1 with two affected females. In the affected male of family 2, we found this variant in a compound heterozygous state together with a novel frameshift variant (c.329\_332delTCTG, p.Leu112Valfs\*8), which is the second frameshift variant known so far in *PYROXD1*. We have been able to define a large homozygous region in family 1 sharing a common haplotype with family 2 in the critical region. Our data suggest that c.464A>G is a Turkish founder mutation. To gain deeper insights, we performed a systematic review of all published *PYROXD1*-related myopathy cases. Our analysis showed that the c.464A > G variant was found in 87% (20/23) of the patients and that it may cause either a childhood- or adult-onset phenotype, irrespective of its presence in a homozygous or compound heterozygous state. Interestingly, only four patients had elevated CK levels (up to 1000 U/L), and cardiac involvement was found in few compound heterozygous cases.

## KEYWORDS

congenital myopathy, haplotype analysis, LGMD, Mendeliome, *PYROXD1*, whole exome sequencing

## 1 | INTRODUCTION

The congenital myopathies (CMs) are a heterogeneous group of rare hereditary muscle diseases manifesting with hypotonia and muscle weakness pre- or perinatally and are characterized histopathologically by distinctive structural lesions within the skeletal muscle (Walton & Nattrass, 1954). CMs have been classified into five subgroups based on the predominant structural pathological hallmarks present on skeletal muscle biopsies: core myopathies, nemaline myopathies, centronuclear myopathies, congenital fiber-type disproportion myopathy, and myosin storage myopathy (Claeys, 2020; Scoto et al., 2013; Wang et al., 2018). This histopathological classification has been amended by the etiological classification based on the associated (mutated) gene since the underlying causal defects leading to CMs are Mendelian gene mutations (Claeys, 2020).

One of the latest identified disease-associated genes for CMs presenting with overlapping clinical and histopathological features of core, centronuclear, myofibrillar, and nemaline myopathies is the *pyridine nucleotide-disulfide oxidoreductase domain 1* (*PYROXD1*) gene (O'Grady et al., 2016). The first publication of the phenotypes associated with pathogenic variants in *PYROXD1* revealed an early-onset myopathic disease with slow progression but also with signs of dystrophy in the muscle biopsies and myofibrillar alterations, mostly in families with Turkish origin (O'Grady et al., 2016). Subsequent publications revealed *PYROXD1* variants causing congenital myopathy but, interestingly, showing that patients with an adult-onset muscular dystrophy phenotype as well (Lornage et al., 2019; O'Grady et al., 2016; Saha et al., 2018; Sainio et al., 2019) are having the same variant c.464A>G, p.Asn155Ser in a homozygous or compound heterozygous state. Thus, the genotype–phenotype correlation of *PYROXD1*-related primary muscle disease has not been well understood because of the wide clinical spectrum of reported phenotypes.

In this report, we describe three Turkish cases presenting with an early-onset and slow progression of muscle weakness. We performed detailed clinical, genetic, and histopathological investigation. To enhance our understanding of the *PYROXD1*-related myopathies, we performed a systematic review of all published cases. These findings prompted us to investigate if this particular variant could be a founder mutation in families of Turkish descent. Indeed, haplotype analyses confirmed that c.464A>G is a founder mutation in the Turkish population.

## 2 | MATERIAL AND METHODS

### 2.1 | Histopathology studies

The muscle biopsy at the age of 12 years from Patient 1 (Yis et al., 2018) and at the age of 8 years from Patient 3 was processed with standard techniques and was analyzed histologically as described elsewhere (Dubowitz & Sewry, 2013). Additionally, immunohistochemistry was performed using myotilin antibody (Novocastra, UK, NCL-myotilin), and the neonatal myosin heavy chain antibody (Novocastra, UK, NCL-MHCn) was used for the identification of immature fibers (further details in Supplementary Data [Appendix S1]).

### 2.2 | Genomic analyses

For Patient 3, initially we performed Mendeliome sequencing with Illumina TruSight One (Illumina, San Diego, California, USA) on an Illumina HiSeq 2000 (Wunderlich et al., 2018), but no convincing pathogenic variant could be identified. Later, we used the Agilent SureSelect V6 enrichment kit for whole-exome sequencing (WES) on a HiSeq 4000 sequencer (Illumina, USA) for Patients 1 and 3 with a paired-end 76-bp sequencing protocol according to the manufacturer's recommendations (Wang et al., 2018). Data analysis for both patients was performed with the in-house software Varbank of the Cologne Center for Genomics (Dafsari et al., 2019; Pergande et al., 2020). In brief, technical details on data analysis and variant filtering are given in the Supplementary Data (Appendix S1). Variants were filtered for rare (minor allele frequency 0.1%) homozygous variants (allele read frequency of 75%–100%) in accordance with the expected autosomal recessive mode of inheritance and the known consanguineous background for both patients, as well as for compound heterozygous constellations for both patients. Variants were classified based on their potential pathogenicity (Supplementary data [Appendix S1]). Sanger sequencing was used for the validation of candidate variants in *PYROXD1* and *TTN* (data not shown) as well as cosegregation analysis.

### 2.3 | Systematic literature survey and statistical analyses

We have performed descriptive statistical analysis for all *PYROXD1* patients published in PUBMED (<https://www.ncbi.nlm.nih.gov/pubmed/>) including the three patients reported here (Lornage et al., 2019; O'Grady et al., 2016; Saha et al., 2018; Sainio et al., 2019) (further details are given on methods in Supplementary data [Appendix S1]).

### 2.4 | Haplotype analysis

For haplotype analysis of the mutation NM\_024854.3:c.464A>G (GRCh37/hg19) on chromosome 12 at cytoband p12.1 (chr12:21452130A>G), microsatellite markers were genotyped by PCR with fluorescently labeled primers (Supplementary Table 6–8) and subsequent fragment analysis performed on an ABI 3730XL sequencer (Applied Biosystems). GeneMarker software (Gene Marker Version 1.51) was used for allele calling. Single nucleotide polymorphisms (SNPs) were genotyped by Sanger sequencing of all family members (Supplementary Figure 2–6). For both families (Figure 3), haplotypes were reconstructed manually and visualized with HaploPainter version 1 (further information is given in Supplementary data [Appendix S1]).

## 3 | RESULTS

### 3.1 | Clinical description

Patient 1 was a 17-year-old female and the sixth child of Turkish consanguineous parents (Table 1). The sibling of Patient 1, who is the

TABLE 1 Overview of PYROXD1 patients

ID	Genetic variant	Ethnicity (paper)	Consanguinity	Current age/age of onset [y]	Muscle weakness	High CK	Cardiac involvement	Facial weakness	Swallowing difficulty	Speech difficulty	Ptosis	Respiratory involvement	Neuropathy signs (Hyporeflexia)	Others
1a	c.285 + 1G > A c.1116G > C, p. (Gln372His)	European (Grady et al.)	N	29/5	Symmetrical, axial	N	Y	Y	N	Y	N	Y (15y)	Reduced or absent	N
1b	c.285 + 1G > A c.1116G > C, p. (Gln372His)	European (Grady et al.)	N	26/8	Symmetrical, axial	Y (up to 1000 U/ L)	N	Y	N	Y	N	N	Reduced or absent	N
2a	c.464A > G, p. (Asn155Ser)	Persian - Jewish (Grady et al.)	N	7/infantile	Symmetrical, axial	N	Y	Y	Y	Y	N	N	Reduced or absent	N
2b	c.464A > G, p. (Asn155Ser)	Persian - Jewish (Grady et al.)	N	9/6	Symmetrical, axial	N	N	Y	Y	Y	N	N	Reduced or absent	N
3	c.464A > G, p. (Asn155Ser)	Turkish (Grady et al.)	Y	15/4	Symmetrical	N	Y	Y	N	Y	N	N	Reduced or absent	N
	c.1159_1160 insCAAA,													
4	c.464A > G, p. (Asn155Ser)	Finnish (Sainio et al.)	N	65/49	Proximal, distal abnormal	N	N	N	N	N	N	Y, FVC 54% (63y)	Normal	ambulant needs help rising up
	c.1061A > G, p. (Tyr354Cys)													
5a	Hom., c.464A > G, p. (Asn155Ser)	Turkish (Grady et al.)	Y	31/10	Symmetrical, axial	Y (up to 700 U/L)	N	Y	N	Y	N	N	Reduced or absent	N
5b	Hom., c.464A > G, p. (Asn155Ser)	Turkish (Grady et al.)	Y	21/10	Symmetrical, axial	Y (up to 800 U/L)	N	Y	N	Y	Mild	Y	Reduced or absent	N
6a	Hom., c.464A > G, p. (Asn155Ser)	Turkish (Grady et al.)	Y	22/2	Symmetrical, axial	Y (up to 700 U/L)	N	Y	N	Y	Mild	N	Reduced or absent	N
6b	Hom., c.464A > G, p. (Asn155Ser)	Turkish (Grady et al.)	Y	17/2.5	Symmetrical, axial	Y (up to 376 U/L)	N	Y	N	Y	Mild	N	Reduced or absent	N
7	Hom., c.464A > G, p. (Asn155Ser)	Sudanese (Saha et al.)	Y	37/9	proximal symmetrical	N	N	N	N	N	N	NA	NA	N
8	Hom., c.464A > G, p. (Asn155Ser)	Finnish (Sainio et al.)	N	65/10	Myopathic changes, atrophic upper back muscles	Y (up to 340 U/L)	N	Y	NA	N	Mild	Episodic dyspnea, FVC 40% (64y)	Normal	Ambulant with two sticks.
9a	Hom., c.464A > G, p. (Asn155Ser)	Finnish (Sainio et al.)	N	70/30	Myopathic changes in proximal and paraspinal muscles, neck flexor	N	Y, Two strokes (61y and 66y)	N	N	hoarseness in his voice	N	FVC 67% with severe reduced MIP, MEP and PCF (70y)	Normal	Ambulant with two sticks for 200 m.
9b	Hom., c.464A > G, p. (Asn155Ser)	Finnish (Sainio et al.)	N	70/33	Myopathic changes in proximal, neck flexor	N	N	N	N	N	N	FVC 30%, death due to respiratory insufficiency (68y)	Normal	Wheelchair bound at 66y and deceased at 70y.

TABLE 1 (Continued)

ID	Genetic variant	Ethnicity (paper)	Consanguinity	Current age/age of onset [y]	Muscle weakness	High CK	Cardiac involvement	Facial weakness	Swallowing difficulty	Speech difficulty	Ptosis	Respiratory involvement	Neuropathy signs (Hyporeflexia)	Others
10	c.285 + 1G > A, c.464A > G, p.(Asn155Ser)	France (Lornage et al.)	N	NA/ neonatal	Axial, wheelchair bound since age of 12y	NA	NA	N	NA	Y	NA	NIV and oxygen therapy since 14	Low ears, high-arched feet	Delayed motor milestones and wheelchair bound since the age of 12 years.
11	Hom., c.464A > G, p.(Asn155Ser)	France (Lornage et al.)	Y	66/ childhood	Axial, lower and upper limbs	NA	NA	NA	NA	NA	NA	Reduced VC with 68%	NA	Walking and running difficulties.
12	c.415-976A > G, c.1116G > C, p.(Gln372His)	France (Lornage et al.)	N	Teenager/ neonatal	Proximal, distal, upper and lower limbs, wheelchair-bound since age 13	NA	NA	NA	NA	N	NA	Respiratory insufficiency requires NIV, and oxygen therapy since 14y of age	Y	Delayed motor milestones and wheelchair bound since 12 years of age. Younger brother same genotype died at 16 years of age.
13a	Hom., c.464A > G, p.(Asn155Ser)	Turkish (Reported here)	Y	17/6	Symmetrical more proximal but also shows distal	N (75 U/L)	N	Y	Y	Y	Mild	Sleep hypoventilation	N	N
13b	Hom., c.464A > G, p.(Asn155Ser)	Turkish (Reported here)	Y	38/NA	NA	NA	N	NA	NA	NA	NA	NA	N	N
14	c.464A > G, p.(Asn155Ser) c.329_332delTCTG, p.(L112Vfs*8)	Turkish (Reported here)	Y	8/3	Lower and upper proximal	N (49 U/L)	N	Y	Y	Y	NA	NA	Polynuropathy	N
15	Hom., c.464A > G, p.(Asn155Ser)	Persian-Jewish (Woods et al., 2020)	Y	46/30-33	Proximal	N	N	N	Y	N	N	N	Normal	Sparing of the rectus femoris on magnetic resonance imaging

(Continues)

TABLE 1 (Continued)

ID	Genetic variant	Ethnicity (paper)	Consanguinity	Current age/age of onset [y]	Muscle weakness	High CK	Cardiac involvement	Facial weakness	Swallowing difficulty	Speech difficulty	Prosis	Respiratory involvement	Neuropathy signs (Hyporeflexia)	Others
16	Hom., c.464A > G, p. (Asn155Ser)	Persian-Jewish (Woods et al., 2020)	NA	82/50s	Difficulty climbing stairs	NA	N	N	N	N	N	N	Normal	NA
17	Hom., c.464A > G, p. (Asn155Ser)	Persian-Jewish (Woods et al., 2020)	NA	78/50s	Difficulty climbing stairs	NA	N	N	N	N	N	N	Normal	NA

Note: All patients are listed with an ID number, the genomic result, and ethnicity and referring to described publication. The current age in years means the current age at publication. Available clinical aspects of the patients were compared for further statistical analysis. In total, 20 patients were described; 12 of them are sibling pairs and labeled with "a" and "b."  
Abbreviations: N, no; NA, not available; NIV, noninvasive ventilation; VC, vital capacity; Y, yes.

oldest child, was a 38-year-old female (Patient 2), still alive and walking with support, presenting same phenotype as her sister according to the reporting parents. The fifth child and brother of Patients 1 and 2 (Figure 2(a)-1: 1:II-5) had died at the age of 14 years (y) due to cardiomyopathy. No material of the brother was available for any genomic analyses. Patient 1, the youngest of six children, had normal perinatal history, and motor milestones were normal. Clinical examination at the age of 12 years showed a generalized reduction in the muscle bulk, symmetrical more proximal, but also showed distal muscle weakness with Gowers' sign (Supplementary: Video 1), neck weakness and scapular winging. The creatine kinase (CK) value was normal: 75 IU/L (0–171). The deep tendon reflexes (biceps, triceps, patella, and Achilles) were absent. She started walking at 12 months of age; the first signs of muscle weakness were observed at the age of 6 years. There was mild joint laxity in the upper extremities, and no contractures were observed. She was still ambulant now at the age of 18 years. Furthermore, the patient had facial weakness, nasal speech, and mild difficulties in swallowing, without ophthalmoplegia. Nerve conduction velocities and amplitudes were normal in the left median, ulnar, and peroneal motor nerves. Sensory nerve conduction velocities and amplitudes of left median, ulnar, and sural nerve were also normal. Electromyography of left tibialis anterior, left quadriceps femoris, and right biceps muscles revealed myopathic motor unit potentials. No signs of cardiac dysfunction have been observed until now. Her cognitive and speech development was normal according to her age.

Patient 3 was an 8-year-old boy who was the first and only offspring of consanguineous (first-degree cousins) Turkish parents (Figure 1(a)-(c)). He was diagnosed at the age of 8 years with congenital myopathy with normal CK level (41 IU/L). The patient had difficulties in walking due to his falls, and he could only climb the stairs with help. Clinical examination at the age of 7 years showed a myopathic expression in a long and narrow face, large ears (Figure 1(a)), a thin hand, and long flexible fingers (Figure 1(b),(c)). The total muscle mass was decreased, but the cranial nerve examination was normal at that time. In addition, he had facial weakness, nasal speech, and difficulties with swallowing. The patient had neck muscle weakness and lower and upper proximal weakness. Myotonic reactions could not be elicited, and the cranial magnetic resonance imaging was normal. The diagnostic molecular genetic testing for fragile X syndrome was negative. At the age of 8 years, the nerve conduction velocity showed axonal neuropathy changes that were interpreted as polyneuropathy. He did not show any clinical signs of cardiomyopathy.

### 3.2 | Muscle biopsy findings

A muscle biopsy (Table 2) was carried out for both patients (Figure 1(d)-(h), Supplementary Figure 1(a)-(d)). An incisional biopsy from the deltoid muscle of patient 1 (Figure 1(d)-(h)) showed degenerative myopathic changes in H&E staining including fiber size variability, multiple internalized nuclei, atrophic fibers, and increased fibrous connective tissue (Figure 1(d)). NADH-TR staining showed cores in the muscle fibers (Figure 1(e)). Nemaline rods were not detected by

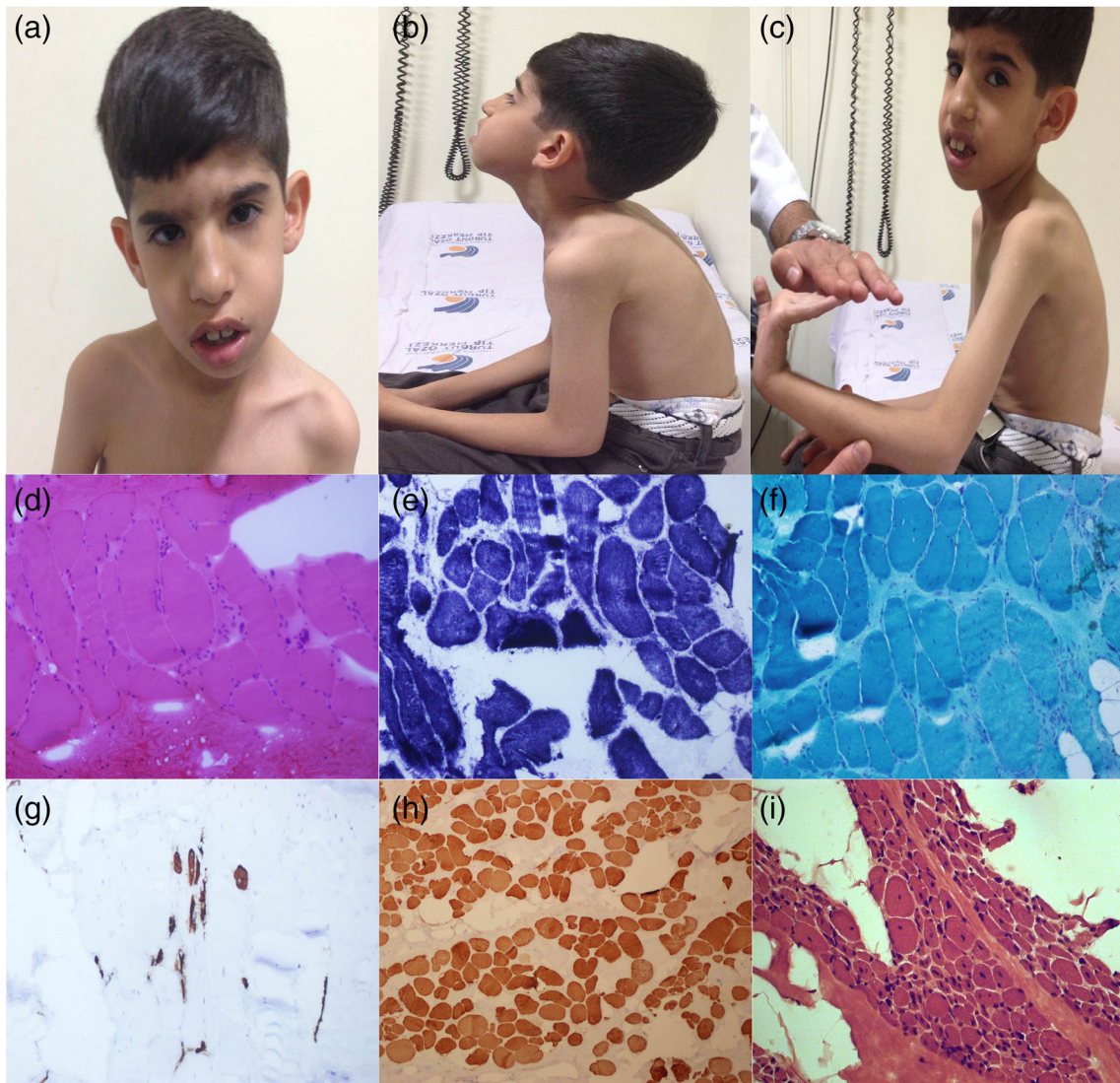


**FIGURE 1** Patient phenotype and muscle biopsy. (a)–(c) Phenotype of patient 3: (a) Long myopathic face and facial weakness. (b) Muscle atrophy of shoulder and neck muscles (c) Distal joint laxity. (d)–(i) Muscle Biopsy for patient 1: (d) Muscle biopsy shows the variation in fiber size, multiple internalized nuclei, and increased fibrous connective tissue (HE  $\times 400$ ), (e) Conspicuous central core formations and myofibrillar irregularity (NADH-TR  $\times 400$ ), (f) Note the increased number of central nuclei (Modified Trichrome  $\times 400$ ), (g) Immature regenerating fibers expressing neonatal myosin (DAB  $\times 400$ ), (h) There are a few central inclusions highly immunoreactive to myotilin. (Scale bars = 25  $\mu\text{m}$ ) (i) Patient 3 muscle biopsy shows severe fatty infiltration, variation in fiber size with a predominance of atrophic fibers and internal nuclei in most fibers. An increase in endomysial connective tissue is also present (H&E stain). More stainings of Patient 3 are shown in Supplementary Figure 1 [Color figure can be viewed at [wileyonlinelibrary.com](http://wileyonlinelibrary.com)]

modified trichrome (Figure 1(f)). Neonatal myosin staining showed immature and regenerating fibers (Figure 1(g)). There were a few central inclusions expressing myotilin (Figure 1(h)). Type 2 myofibers were slightly decreased in the fast and slow myosin heavy chain staining. All the other immunohistochemical analysis showed no abnormalities (Supplementary Data [Appendix S1]). Muscle biopsy results indicated a noninflammatory myopathy.

Patient 3 had a muscle biopsy (Supplementary Figure 1(a)–(d)) performed at the age of 7 years, which showed dystrophic changes. H&E staining (Supplementary Figure 1(a),(b)) represented the presence of abundant small rounded muscle fibers with centrally located nuclei and a noticeable increment of fat tissue in the sections. The patients'

muscle biopsy clearly showed dystrophic changes with increased connective tissues within endo- and perimysium and irregular desmin aggregates in sarcoplasm (Supplementary Figure 1(c),(d)).

### 3.3 | Genomic and haplotype results

For Patient 1 (Figure 2(a)), WES analysis revealed a homozygous variant in *PYROXD1* (NM\_024854.3), c.464A>G causing p.Asn155Ser (Figure 2(c),(d)). The variant had already been published as pathogenic (O'Grady et al., 2016) and reported in the Exome Variant Server (seven heterozygous cases), gnomAD (AF:0.00004624), the general

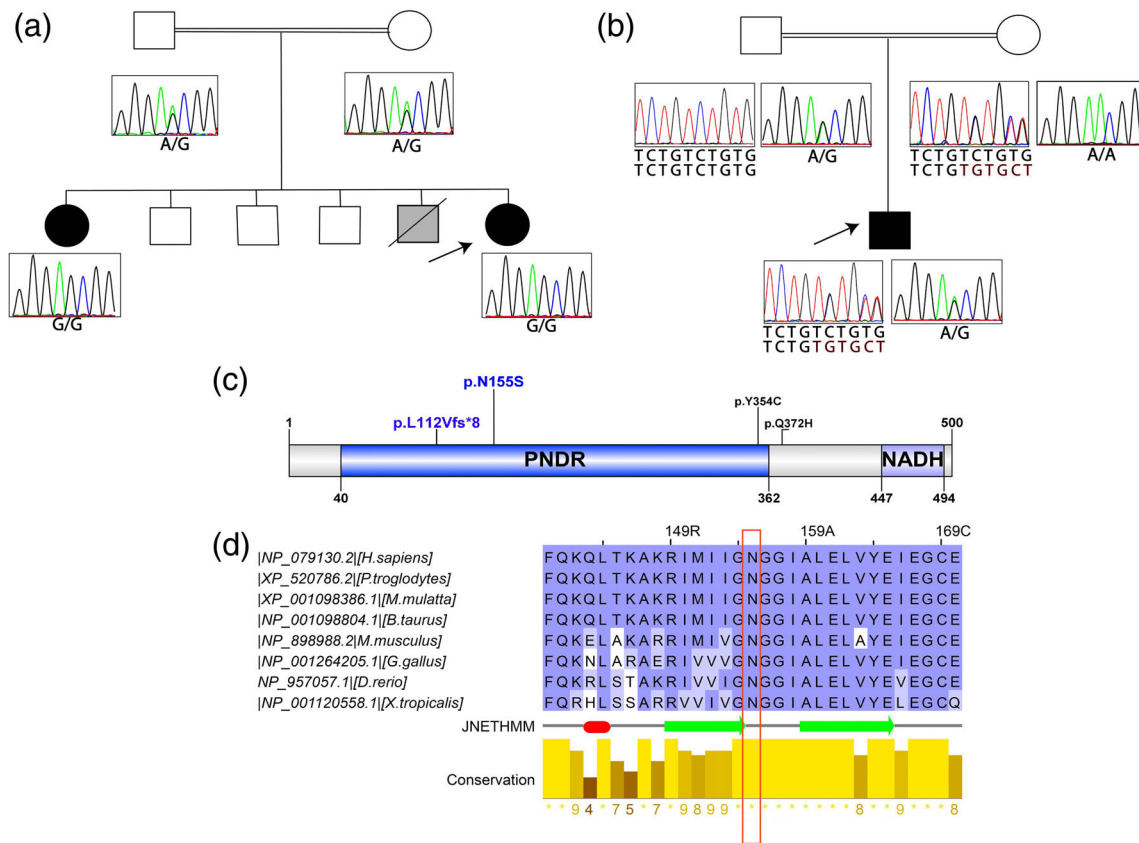


**FIGURE 2** Genomic analysis and protein domain scheme. (a),(b) Pedigrees and cosegregation of family 1 (a) with patient 1 (II:6) and patient 2 (II:1) and family 2 (b) with patient 3 (II:1). Patient 1 (II:6) clearly shows a homozygous variant (red arrow) in *PYROXD1* (c.464A>G, p.Asn155Ser), and her older sister is affected and has the same variant. Both parents are heterozygous for this variant. Patient 3 has two variants in *PYROXD1*, c.464A>G, p.Asn155Ser and c.329\_332del, p.Leu112Valfs\*8. The father (c.464A>G, p.Asn155Ser) and the mother (c.329\_332del, p.Leu112Valfs\*8) of patient 3 are heterozygous for one of the two variants in *PYROXD1*. (c) Protein structure of *PYROXD1*, which has two important domains, the nuclear-cytoplasmic pyridine nucleotide-disulfide reductase (PNDP) domain (shown in purple) and the NADH-dependent nitrite reductase (NADH) domain (shown in rose). The most common variant in *PYROXD1* is p.Asn155Ser (blue); other found missense mutations are p.Tyr354Cys (purple) and p.Gln372His (green). The here reported novel frameshift mutation is shown in red. Three of the variants are located in the PNDP domain of *PYROXD1*. (d) The variant p.Asn155Ser is conserved through evolution in different species: 1. *Homo sapiens* (NP\_079130.2), 2. *P. troglodytes* (XP\_520786), 3. *Macaca mulatta* (XP\_001098386.1), 4. *Bos taurus* (NP\_001098804), 5. *Mus musculus* (NP\_898988), 6. *R. rattus* (NP\_001004234), 7. *Gallus gallus* (NP\_001264205), 7. *Danio rerio* (NP\_957057.1), and 8. *Xenopus tropicalis* (NP\_001120558.1). For our alignment, we used NCBI FASTA files of the different species and add this to Jalview alignment with MuscleWS using service hosted at <http://www.compbio.dundee.ac.uk/jabaws> (MuscleWS version 3.8.31). Afterward, secondary structure analysis on alignment was done by using JPred secondary structure analysis in Jalview, seen in here as JNetHMM. The helices are marked as red tubes and the  $\beta$ -sheets as green arrows in the alignment. At the end, we used a color scheme, here Blossum62, which uses white for gaps, dark purple for residues matches the consensus sequence residue, and light purple for not matching to consensus residue, but the second residue does. The consensus is also displayed in yellow from the lowest (0) to the highest one (10) [Color figure can be viewed at [wileyonlinelibrary.com](http://wileyonlinelibrary.com)]

minor allele frequency without any homozygous cases, and in ClinVar (Supplementary Table 2–3). This variant was classified as pathogenic by the ACMG standards and criteria guidelines (Richards et al., 2015), and it is conserved through evolution (Figure 2(d)). In addition, our filtering results revealed different *TTN* variants in Patient 1 (Supplementary Table 3), which were excluded by lack of cosegregation (data not shown).

Mendeliome sequencing based on the gene list of 2013 (Wunderlich et al., 2018) did not reveal any pathogenic variants because *PYROXD1* was not included in the panel. WES for Patient 3 (Figure 2(b)) revealed compound heterozygous mutations in

*PYROXD1* (Figure 2(c),(d)); in addition to mutation c.464A>G, p.Asn155Ser, a novel frameshift variant c.329\_332delTCTG, p.Leu112Valfs\*8 was found (Supplementary Table 3), which was not reported in the Exome Variant Server, gnomAD, Great Middle Eastern database (GME), Iranome, ClinVar and 1000 genomes databases (Supplementary Tables 4 and 5). We classified this variant as likely pathogenic (Richards et al., 2015).

Haplotype analysis around the c.464A>G, p.Asn155Ser (chr12:21605064A>G) variant (Supplementary Table 9–10) was performed for both families of Turkish origin. We proved that both families share a haplotype of 282,729 bp (Figure 3 Family 1–2, red boxes). In Family

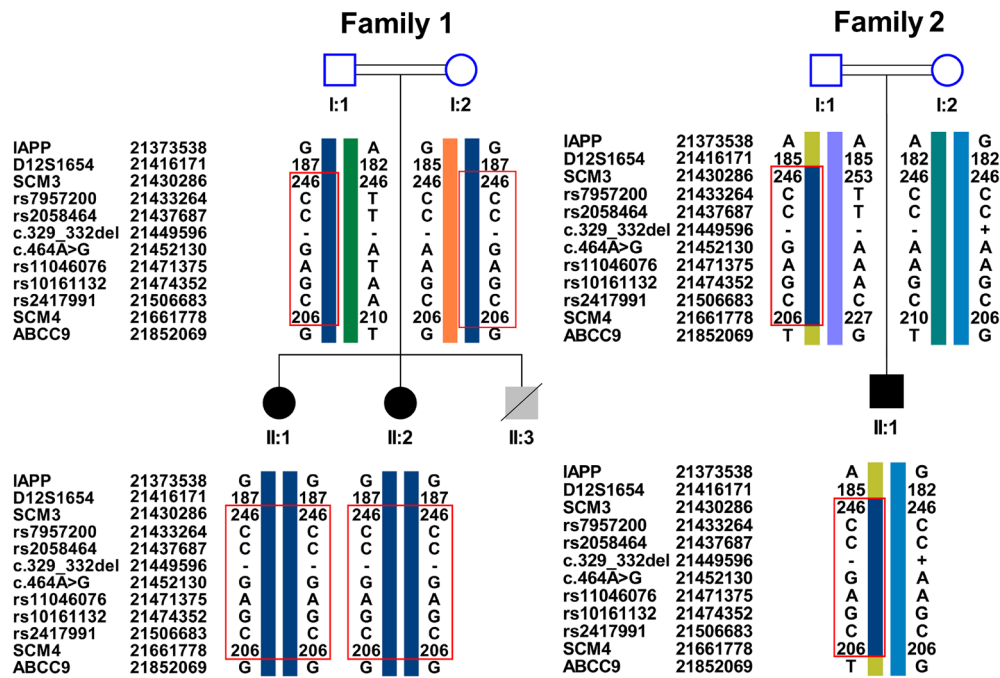


**FIGURE 3** Haplotypes of family 1 and family 2. Representation of the haplotypes (GRCh37/hg19) determined for individuals with the NM\_024854.3:c.464A > G (12:21452130), variant at chromosome region 12p12.1. In Figure 3, both families' haplotypes, family 1 and family 2, were presented. For Family 1, we only showed the two female siblings (II:1 and II:2) and the deceased brother, and not included the healthy siblings, because DNA was not available for genotyping. Haplotypes were reconstructed manually from the genotypes of following markers: IAPP (12:21373538 A > G) (SNV); D12S1654 (STR); SCM3 (12:21583220–21,583,464) (STR); rs7957200 (SNV); rs2058464 (SNV); rs11046076 (SNV); rs10161132 (SNV); rs2417991 (SNV); SCM4 (12:21661778–21,661,981) (STR); and ABCC9, (12:21852069 T > G) (SNV), and were visualized by the HaploPainter software. The first column shows the name of the markers, and the second column shows the allelic position on chromosome 12. Each number on haplotypes represents different alleles for a microsatellite marker, and the letters represent different alleles for each SNV. The NM\_024854.3:c.329\_332delTCTG (12: 21602540\_21602543delTCTG) is the second compound heterozygous mutation in Family 2; the “+” indicates the deletion and the “-” indicates the wt allele without deletion. The shared founder haplotype for *PYROXD1* c.464A > G between the individuals is marked with a red box. The analysis of the two families revealed 231,492 bp homozygous region in patients from the marker D12S1654 (12:21569340) to the ABCC9 SNV [Color figure can be viewed at [wileyonlinelibrary.com](http://wileyonlinelibrary.com)]

1, we found the same haplotype heterozygous in both parents and homozygous in the two affected siblings (Patients 1 and 2 in Figure 3, Family 1). No DNA material of the other three healthy siblings was available (healthy siblings are not shown in Figure 3 and Supplementary Figure 2–6). In the second family, Patient 3 has a second mutation in *PYROXD1* that causes a frameshift by a deletion (Figure 3, Family 2). Clearly, we have been able to show the heterozygous haplotype together with the missense variant in this family too (Figure 3, red boxes), except the mother. These findings proved the variant c.464A>G as a Turkish origin founder mutation. Comparing the genomic data including SNVs of our two patients with the published haplotype region in three Turkish families in the publication of O'Grady (O'Grady et al., 2016) revealed the same homozygous region in all Turkish families. Furthermore, we discovered a larger homozygous region in our patients by adding our microsatellites and SNP positions to the already found homozygous region in the five families. Conclusively, our analysis not only showed that c.464A>G is a founder mutation in the Turkish population, but a shared homozygous region with earlier published cases was also discovered here, indicating an identity-by-descent of this mutation in the analyzed cases (Supplementary Table 10).

### 3.4 | Statistical results of systematic literature survey

The statistical analysis of the 23 included individuals shown in Table 3 (Lornage et al., 2019; O'Grady et al., 2016; Saha et al., 2018; Sainio et al., 2019) revealed that the current median age of the patients by the phenotypes is 15y, with age range from 7 to 22y for the early-onset patients, and 65 year for the adult ones, with an age range from 26 to 82 year. It represents the current age by different age groups, leading to a childhood-teenage group with an average age of 12.5 year ( $n = 7$ ), adult age group with 31 year ( $n = 8$ ), and an old age group with 72 year ( $n = 5$ ) as current age. The age of onset of the patients, including all patients with and without the founder mutation can be divided in three groups, starting with the early-onset patients with an age range from neonatal up to 3 year resulting in an average age onset of 1.5 year ( $n = 11$ ). The second group, the childhood-onset patients, has an age range from 4 to 10 year, resulting in an average age of 7.4 year ( $n = 10$ ), and the adult-onset patients demonstrate an average age of onset of 32 year ( $n = 6$ ). It was found that the youngest age of onset occurred during the neonatal period and the oldest one at 50 year of age, and both the cases are carrying founder mutation.



**TABLE 2** Muscle biopsy results

ID	Age at biopsy	Internalized nuclei	Central cores	Myofibrillar inclusions	Sarcomeric disorganization	Thin filament accumulations	Nemaline rods	Fiber size variability	Fatty replacement	Increased fibrosis	Biopsy
13a	12y	Y	NA	Y	NA	NA	Y	Y	Y	Y	Myopathic changes
14	8y	Y	Y	Y	NA	Y	NA	Y	Y	Y	Myopathic changes
1a	11y	Y	Y	Y	Y	Y	Y	Y	Y	Y	Myopathic changes
2a	4y	Y	Y	Y	Y	N	N	Y	Y	Y	Myopathic changes
3	10y	Y	Y	n.p.	N	N	N	Y	Y	Y	Myopathic changes
5a	16y	Y	Y	Y	Y	Y	Y	NA	Y	Y	Myopathic changes
6a	13y	Y (>50% of fibers)	Y on NADH and SDH stains	N	N	N	N	NA	Y	Y	Myopathic changes
4	NA	NA	NA	NA	NA	NA	NA	Y	Y	NA	Dystrophic
8	NA	NA	NA	NA	NA	NA	NA	Y	Y	NA	Dystrophic
9a	70y	NA	NA	NA	NA	NA	NA	Y	Y	NA	Dystrophic
10	6y	Y	Y	Y	Y	N	Y	Y	N	Y	Myopathic changes
11	26y and 66y	Y	Y	Y	Y	N	Y	Y	N	Y	Myopathic changes
12	6y	Y	Y	Y	Y	N	N	Y	N	Y	Myopathic changes
15	37y	Y	Y	Y	Y	Y	Y	Y	NA	N	Myopathic changes

Note: The muscle biopsy results of published and here reported patients, in total 70% (14/20) of all patients, had a muscle biopsy. Patient ID matches the numbers in Table 1. In general, the biopsy was performed at a teenage age (age at biopsy), except Finnish patients because of their late onset. Most important aspects of the muscle biopsy results were listed and compared. Importantly, the fiber size variation, internal nuclei, fatty replacement, and fibrosis were listed. Furthermore, if central cores were observed, any sarcomeric disorganization, myofibrillar inclusions, or thin filament accumulations occurred. This information summarized showed dystrophic (patient 4, 8, 9a) or myopathic changes. Abbreviations: N, no; NA, not available; Y, yes.

**TABLE 3** Statistical analysis of systematic literature survey

Patients	23 (100%)
Ethnicity	34.5% Turkish, 8.7% European, 21.7% Persian-Jewish, 17.4% Finnish, 4.4% Sudanese, 13.3% France
Consanguinity	47.8%
Current median age of patients by phenotype in years (y) (n = 23)	I. Early-onset (onset of disease until 6y): 15y (age range from 7 to 29y), II. Adult-onset (onset of disease after 6y): 65y (age range from 26 to 82y)
Current mean age of patients by age-groups in years (y) (n = 23)	I. Childhood-teenager (7-17y):12.5y (n = 7), II. Adult age (21-46y): 31y (n = 8), III. Old age (65-82y): 72y (n = 5)
Average age of onset in years (y)	I. Early onset up to 3y:1.5y (n = 11), II. Childhood onset (up to 10y):7.4y (n = 10), III. Adult onset (up to age 50y):32y (n = 6)
Homozygous patients (c.464A > G, p.Asn155Ser)	61% (n = 14)
Compound heterozygous patients / of them with founder mutation	39% (n = 9) / 26.1% (n = 6)
CK elevated (range 340-1000 U/L)	26% (n = 6)
Cardiac involvement	17.4% (n = 4)
Facial weakness	52.2% (n = 12)
Swallowing difficulty	21.7% (n = 5)
Speech difficulty	52.2% (n = 12)
Ptosis	21.7% (n = 5)
Respiratory involvement	43.5% (n = 10)
Neuropathic signs	47.8% (n = 11)
Muscle biopsy	60.8% (14/23)
Average age at biopsy	22y (n = 12)
Average age at biopsy classified in	1. Until teenage age = 9.5y (n = 9), 2. Middle age = 37y (n = 1), 3. Older age = 68y (n = 2)
Internalized nuclei	78.6%
Central cores	71.4%
Myofibrillar inclusions	64.3%
Sarcomeric disorganization	50%
Thin filament accumulation	28.6%
Nemaline rods	42.6%
Fiber size variability	85.7%
Fatty replacement	71.4%
Increased fibrosis	71.4%
Overall muscle biopsy evaluation reported	79% myopathic, 21% dystrophic

Note: This overview shows the statistical analysis of the patients with general aspects (ethnicity and age), clinical factors including age of onset, cardiac involvement, weakness and difficulties of patients, and biopsy results.

The age of onset of the three patients without the founder mutation was neonatal or in childhood. The percentage of the patients who are homozygous for the founder mutation are 61% (n = 14), and 39% are compound heterozygous (n = 9), with 26.1% (n = 6) of them having the founder mutation. The founder mutation is the only one found in homozygous state in all reported patients with *PYROXD1*.

The most common clinical features of *PYROXD1*-mutated patients are facial weakness (52%), speech difficulties (56.5%), swallowing

difficulties (17.4%), ptosis (21.4%), and high CK levels (26%). Cardiac involvement was only found in 17.4% of the patients, but half of the patients have a respiratory insufficiency (43.8%). Signs of neuropathy were reported in 47.8% of all reported *PYROXD1* patients.

In total, 14 patients out of 23 had a described muscle biopsy (60.8%) (Table 2). In Table 3, the statistical analysis revealed that the patients can be divided into three groups by their age at biopsy, starting with group (I) until the teenage age with a mean age at

9.5 year for 9/14 patients (65%), second group (II) only one patient at the age of 37 year and the last, and third group (III) with a mean age of 68 year including two of 14 patients. Most common features in the muscle biopsy were fiber size variation (85.7%), internalized nuclei (78.6%), central cores (71.4%), myofibrillar inclusions (64.3%), fatty replacement (71.4%), and fibrosis (71.4%). The muscle biopsy changes had been interpreted as myopathic for most of the patients, except the Finnish patients, who were described as dystrophic.

## 4 | DISCUSSION

The genomic analysis of the three patients reported here led us to *PYROXD1* (Figure 2(a)-(d)). We proved that the *PYROXD1* c.464A>G, p.Asn155Ser variant is a founder mutation in the Turkish population, although it was not reported in the GME Variome. The gnomAD database showed six heterozygous individuals in the healthy Finnish and another six heterozygous in the European population harboring the founder mutation. Unfortunately, no Turkish genome database exists. Our own analyses revealed that the three cases reported here were obtained from the 807 exome-sequenced patients, of which 287 were Turkish-origin patients, revealing an allele frequency of 0.0052 (3/574) for the Turkish population calculated from our in-house database. In gnomAD 10.824, Finnish patients have been sequenced, and only six heterozygous individuals were found to harbor the founder mutation, which gives an AF of 0.00055 for the Finnish population. Our haplotype analysis showed a shared haplotype of 231,492 bp spanning the variant c.464A>G, (chr12:21605064A>G) in both families (Figure 3, Family 1 and 2, red boxes). A homozygous haplotype around this variant c.464A>G (chr12:21605064A>G) was also reported by O'Grady et al. in three Turkish families (O'Grady et al., 2016). We compared the genomic data of all five Turkish families (Supplementary Table 10), which revealed the same shared homozygous region of haplotypes (348,622 bp), supporting our findings. A deeper understanding of the spatial patterns of relatedness in subpopulations could be gained by using haplotype analysis on reported *PYROXD1* patients with the c.464A>G mutation.

The founder mutation has a predicted destabilizing effect on *PYROXD1* by the amino acid substitution (Supplementary Figure 7A-C). The used "DynaMut" molecular dynamics prediction (described in Supplementary Data [Appendix S1]) showed that the asparagine at position 155 (Supplementary Figure 7(b), (c)-in green) is located in the  $\alpha$ -helix (H6) of *PYROXD1*. Asparagine maintains the  $\alpha$ -helical structure by several bonds (gray-dashed line) and a main binding to tryptophan (Supplementary Figure 7(b), (c)-green-dashed line) and the red-dashed H-bonds with the peptide backbone. The prediction analysis showed that replacing asparagine by serine which has an OH-group instead of a carboxamide group has a destabilizing effect on the *PYROXD1* structure (Supplementary Figure 7(d), (e) in green).

All published patients are listed in Table 1 and can be divided into (1) individuals with an early-onset phenotype, including facial weakness, nasal speech, and swallowing difficulties, but still ambulant with help and (2) individuals with an adult phenotype alive up to 80 years

of age, showing first symptoms in the 40s or even 50s with no cardiac involvement, normal CK levels, and no facial weakness (O'Grady et al., 2016; Saha et al., 2018). The founder mutation c.464A>G has been reported to cause two different phenotypes, (i) and (ii), and it was observed either in homozygous (14/23, 61%) or compound heterozygous (6/23, 26%) state.

The Turkish founder mutation was reported in total in 14/23 (61%) patients in homozygous state; six of them have been Turkish-origin patients. All of the Turkish-origin patients were consanguineous, showed high CK levels, facial weakness (6/6), and speech difficulties (6/6). The Turkish patients also had mild ptosis (4/6), one with respiratory insufficiency (1/6) and nearly all having neuropathy signs (5/6). The non-Turkish patients showed less frequent facial weakness (1/8), speech difficulties (2/8), and ptosis (1/8), but respiratory insufficiency was found in 50% of this subgroup of patients (4/8). The age of onset in the homozygous group of all populations suggests the division in two groups, one early to childhood, from 2 to 10 years of age, including the Turkish origin patients, and the second group with an older age of onset from 30 to 50 years of age, including mostly Finnish and Persian-Jewish patients.

Only four patients in the cohort were reported with cardiomyopathy and, oddly, three of them having siblings (Table 1, patients: 1b, 2b, and 9b) without cardiac involvement. Each sibling pair has the same genotype. The most likely reason for these discordant cardiac phenotypes could be secondary genetic variants in other genes (genetic modifiers). Cases reported without the founder mutation are all compound heterozygous (3/23) (Table 1). Two of them are European siblings with an essential splice-site mutation (O'Grady et al., 2016), and one of them has a functional deep intronic mutation and is wheelchair bound since the age of 12 year (Lornage et al., 2019). Conclusively, the founder mutation has been the only reported homozygous mutation in *PYROXD1* patients (Table 1, Table 3).

The function of *PYROXD1* is still unknown, but it has been localized to the nucleus and sarcomeres of human muscles and zebra fish (*pyroxd1*) myofibers (O'Grady et al., 2016). *PYROXD1* is a class I pyridine nucleotide-disulfide oxidoreductase (PNDR), predicted to have a flavin adenine dinucleotide (FAD) binding site (O'Grady et al., 2016). Three different isoforms of *PYROXD1* have been described (Supplementary Figure 8 for isoform 1 and 2); besides the longest isoform (isoform 1, NM\_024854.5, ENST00000240651.14, Figure 2(C)), two other isoforms with a shorter N-terminus are existing. Isoform 2 (NM\_001350912.1, ENST00000538582.5) has same domains as isoform 1 and isoform 3 (NM\_001350913.2, data not shown) containing only one domain, the PNDR domain. Isoform 1 is widely expressed among all tissues in comparison with isoform 2, which shows no expression in skeletal muscle (Supplementary Figure 8, red box and arrow). Complementation assays with *PYROXD1* in yeast lacking glutathione reductase have shown its reductase activity and have also shown that the glutathione reductase activity was impaired by the missense mutation c.464A > G, p.Asn155Ser and could be rescued by human wt *PYROXD1* (O'Grady et al., 2016). Glutathione reductase has an important role for the survival of cells against oxidative stress induced by, for example, reactive oxygen species (ROS) (Wu & Batist, 2013).

Recently, *PYROXD2* was reported as a protein localized in the inner membrane of the mitochondria (T. Wang et al., 2019). The knockout of *PYROXD2* led to increased levels of mitochondrial ROS (mtROS) (T. Wang et al., 2019), which is known to cause cellular damage and also to misfolding of mitochondrial proteins (Chandel, Schumacker, & Arch, 2001), indicating that *PYROXD2* is a regulator of the mitochondrial activity and regulates mtROS levels. No functional association between *PYROXD1* and *PYROXD2* was reported yet, but the function of *PYROXD2* as a regulator of mtROS (Wang et al., 2019) and the fact that *PYROXD1* rescued the yeast glutathione reductase knockout in a complementation assay (O'Grady et al., 2016) suggested that *PYROXD1* could be involved in the compensation of oxidative stress in other cellular compartments than mitochondria. Furthermore, high levels of HSP70 and glutathione reductase in patients muscle tissue in Western blot analysis suggested that *PYROXD1* could be also a regulator of autophagy (Lornage et al., 2019) and ROS. *PYROXD1* could be a specific regulator of the ROS in the nucleus by its localization. Interestingly, used online tools predicted a nucleus localization signal sequence for *PYROXD1* from amino acid position 250–282, which predicts a transport to the nucleus by importin-alpha (Supplementary Figure 9), but *PYROXD1* is also in the cytoplasm. Cores were found in the muscle biopsy of *PYROXD1* patients (Figure 1(e)), which was also reported in loss-of-function mutations in *SEPN1* patients muscle fibers (Marino et al., 2015; Scoto et al., 2013), additionally with small focal areas in the mitochondria (Arbogast & Ferreiro, 2010). *SEPN1*, also called *SELENON* (Varone et al., 2019), belongs to the selenoproteome (Arbogast & Ferreiro, 2010) characterized by selenocysteines with no classical FAD or NADH binding domains (Lescure, Gautheret, Carbon, & Krol, 1999). Mutations found in the *SELENON* cause congenital core myopathy phenotypes (Marino et al., 2015; Moghadasszadeh et al., 2001) and are leading to alteration of the antioxidant systems (Arbogast et al., 2009) and  $\text{Ca}^{2+}$  homeostasis (Marino et al., 2015) in muscles. Low levels of ROS and NO are produced in a healthy muscle, important for the excitation–contraction coupling and signal transduction. Higher levels of both, ROS and NO after exercise could lead to oxidative and nitrosative stress in the muscle, if not regulatory mechanism fail, leading to dysfunction or lethality of the myofibers. Arbogast et al., was the first to analyze intracellular oxidant activity in human *SELENON*-mutated fibroblast and myotubes and showed that they contained high levels of oxidized sarcomeric protein in OxyBlot's. These findings indicate a specific disease mechanism of ROS-related myopathies and *SELENON* deficiencies (Arbogast et al., 2009). As we know that *PYROXD1* is a regulator of ROS in the muscle, like *SELENON* (Arbogast et al., 2009), we hypothesize that hyperoxidation of contractile muscle proteins could be a specific disease mechanism for *PYROXD1*-related myopathies. This could be confirmed by utilizing OxyBlot' kit from patients' muscle biopsies. Further research in patient material and in murine models would be required to understand the biological role of *PYROXD1* against oxidative stress in skeletal muscle.

## 5 | CONCLUSION

In this study, we report three patients with an early-onset myopathy due to *PYROXD1* mutations. Our in-depth haplotype analyses proved

that the c.464A>G, p.Asn155Ser substitution is a founder mutation in the Turkish population. Our systematic literature review revealed that the *PYROXD1* missense variant c.464A>G, p.Asn155Ser is the only homozygous *PYROXD1* mutation reported so far and may cause an early- or an adult-onset phenotype, irrespective of if its occurrence either in the homozygous or compound heterozygous state. Cardiac involvement was rare. CK levels in *PYROXD1*-related myopathies were usually below 1000 U/L.

## ACKNOWLEDGMENTS

We thank the patients and their families contributing to this clinical study. This work was supported by the Deutsche Forschungsgemeinschaft, Germany grants (CI 218/1-1) and Köln Fortune Grants to SC. Open access funding enabled and organized by Projekt DEAL.

## CONFLICT OF INTEREST

The authors report no conflict of interest for this manuscript with the title “Clinical and genetic characterization of *PYROXD1*-related myopathy patients from Turkey.”

## AUTHOR CONTRIBUTIONS

Manuscript writing, genetic data and bioinformatics analysis, and sequencing were performed by Hülya-Sevcan Daimagüler. UA contributed to manuscript writing. OO contributed to haplotype analysis, figure generation and manuscript writing. Patient clinical and histopathological observations were collected by Uluc Yis, Serdal Güngör, Beril Talim, Gülden Diniz, and Figen Baydan. Holger Thiele, Janine Altmüller, and Peter Nürnberg provided NGS data. Analysis of WES data, funding, study design, manuscript writing, and supervision of the study was provided by Sebahattin Cirak. All Authors have critically reviewed and approved the manuscript.



## ETHICS STATEMENT

Informed consent was obtained by the families. The genetic study was approved by the local institutional review board of the University Hospital Cologne, and informed consent for genetic workup was obtained from the patients and family members.

## DATA AVAILABILITY STATEMENT

The data that support the findings of this study are available from the corresponding author upon reasonable request.

## ORCID

Hülya-Sevcan Daimagüler  <https://orcid.org/0000-0001-8874-8125>  
Özkan Özdemir  <https://orcid.org/0000-0002-2647-6416>

## REFERENCES

- Arbogast, S., Beuvin, M., Fraysse, B., Zhou, H., Muntoni, F., & Ferreiro, A. (2009). Oxidative stress in *SEPN1*-related myopathy: From pathophysiology to treatment. *Annals of Neurology*, 65(6), 677–686. <https://doi.org/10.1002/ana.21644>
- Arbogast, S., & Ferreiro, A. (2010). Selenoproteins and protection against oxidative stress: Selenoprotein N as a novel player at the crossroads

- of redox signaling and calcium homeostasis. *Antioxidants & Redox Signaling*, 12(7), 893–904. <https://doi.org/10.1089/ars.2009.2890>
- Chandel, N. S., Schumacker, P. T., & Arch, R. H. (2001). Reactive oxygen species are downstream products of TRAF-mediated signal transduction. *The Journal of Biological Chemistry*, 276(46), 42728–42736. <https://doi.org/10.1074/jbc.M103074200>
- Claeys, K. G. (2020). Congenital myopathies: An update. *Developmental Medicine and Child Neurology*, 62(3), 297–302. <https://doi.org/10.1111/dmcn.14365>
- Dafsari, H. S., Kocaturk, N. M., Daimaguler, H. S., Brunn, A., Dotsch, J., Weis, J., Deckert, M., & Cirak, S. (2019). Bi-allelic mutations in uncoordinated mutant number-45 myosin chaperone B are a cause for congenital myopathy. *Acta Neuropathologica Communications*, 7(1), 211. <https://doi.org/10.1186/s40478-019-0869-1>
- Dubowitz, V., & Sewry, C. (2013). *Muscle biopsy: A practical approach* (4th ed.). Philadelphia, PA: Saunders Ltd.
- Lescure, A., Gautheret, D., Carbon, P., & Krol, A. (1999). Novel selenoproteins identified in silico and in vivo by using a conserved RNA structural motif. *The Journal of Biological Chemistry*, 274(53), 38147–38154. <https://doi.org/10.1074/jbc.274.53.38147>
- Lornage, X., Schartner, V., Balbuena, I., Biancalana, V., Willis, T., Echaniz-Laguna, A., Scheidecker, S., Quinlivan, R., Fardeau, M., Malfatti, E., Lannes, B., Sewry, C., Romero, N. B., Laporte, J., & Böhm, J. (2019). Clinical, histological, and genetic characterization of PYROXD1-related myopathy. *Acta Neuropathologica Communications*, 7(1), 138. <https://doi.org/10.1186/s40478-019-0781-8>
- Marino, M., Stoilova, T., Giorgi, C., Bachi, A., Cattaneo, A., Auricchio, A., Pinton, P., & Zito, E. (2015). SEP1, an endoplasmic reticulum-localized selenoprotein linked to skeletal muscle pathology, counteracts hyperoxidation by means of redox-regulating SERCA2 pump activity. *Human Molecular Genetics*, 24(7), 1843–1855. <https://doi.org/10.1093/hmg/ddu602>
- Moghadaszadeh, B., Petit, N., Jaillard, C., Brockington, M., Quijano Roy, S., Merlini, L., Romero, N., Estournet, B., Desguerre, I., Chaigne, D., Muntoni, F., Topaloglu, H., & Guicheney, P. (2001). Mutations in SEP1 cause congenital muscular dystrophy with spinal rigidity and restrictive respiratory syndrome. *Nature Genetics*, 29(1), 17–18. <https://doi.org/10.1038/ng713>
- O'Grady, G. L., Best, H. A., Sztal, T. E., Schartner, V., Sanjuan-Vazquez, M., Donkervoort, S., Abath Neto, O., Sutton, R. B., Ilkovski, B., Romero, N. B., Stojkovic, T., Dastgir, J., Waddell, L. B., Boland, A., Hu, Y., Williams, C., Ruparella, A. A., Maisonobe, T., Peduto, A. J., ... Cooper, S. T. (2016). Variants in the oxidoreductase PYROXD1 cause early-onset myopathy with internalized nuclei and Myofibrillar disorganization. *American Journal of Human Genetics*, 99(5), 1086–1105. <https://doi.org/10.1016/j.ajhg.2016.09.005>
- Pergande, M., Motameny, S., Özdemir, Ö., Kreutzer, M., Wang, H., Daimagüler, H. S., Becker, K., Karakaya, M., Ehrhardt, H., Elcioglu, N., Ostojic, S., Chao, C. M., Kawalia, A., Duman, Ö., Koy, A., Hahn, A., Reimann, J., Schoner, K., Schänzer, A., Westhoff, J. H., ... Cirak, S. (2020). The genomic and clinical landscape of fetal akinesia. *Genetics in Medicine*, 22(3), 511–523. <https://doi.org/10.1038/s41436-019-0680-1>
- Richards, S., Aziz, N., Bale, S., Bick, D., Das, S., Gastier-Foster, J., Grody, W. W., Hegde, M., Lyon, E., Spector, E., Voelkerding, K., Rehm, H. L. (2015). Standards and guidelines for the interpretation of sequence variants: A joint consensus recommendation of the American College of Medical Genetics and Genomics and the Association for Molecular Pathology. *Genetics in Medicine*, 17(5), 405–424. <https://doi.org/10.1038/gim.2015.30>
- Saha, M., Reddy, H. M., Salih, M. A., Estrella, E., Jones, M. D., Mitsuhashi, S., Cho, K. A., Suzuki-Hatano, S., Rizzo, S. A., Hamad, M. H., Mukhtar, M. M., Hamed, A. A., Elseed, M. A., Lek, M., Valkanas, E., MacArthur, D. G., Kunkel, L. M., Pacak, C. A., Draper, I., & Kang, P. B. (2018). The impact of PYROXD1 deficiency on cellular respiration and correlations with genetic analyses of limb-girdle muscular dystrophy in Saudi Arabia and Sudan. *Physiological Genomics*, 50, 929–939. <https://doi.org/10.1152/physiolgenomics.00036.2018>
- Sainio, M. T., Välipakka, S., Rinaldi, B., Lapatto, H., Paetau, A., Ojanen, S., Brilhante, V., Jokela, M., Huovinen, S., Auranen, M., Palmio, J., Friant, S., Ylikallio, E., Udd, B., & Tyynismaa, H. (2019). Recessive PYROXD1 mutations cause adult-onset limb-girdle-type muscular dystrophy. *Journal of Neurology*, 266(2), 353–360. <https://doi.org/10.1007/s00415-018-9137-8>
- Scoto, M., Cullup, T., Cirak, S., Yau, S., Manzur, A. Y., Feng, L., Jacques, T. S., Anderson, G., Abbs, S., Sewry, C., Jungbluth, H., & Muntoni, F. (2013). Nebulin (NEB) mutations in a childhood onset distal myopathy with rods and cores uncovered by next generation sequencing. *European Journal of Human Genetics*, 21(11), 1249–1252. <https://doi.org/10.1038/ejhg.2013.31>
- Varone, E., Pozzer, D., Di Modica, S., Chernorudskiy, A., Nogara, L., Baraldo, M., Cinquanta, M., Fumagalli, S., Villar-Quiles, R. N., De Simoni, M. G., Blaauw, B., Ferreira, A., & Zito, E. (2019). SELENON (SEP1) protects skeletal muscle from saturated fatty acid-induced ER stress and insulin resistance. *Redox Biology*, 24, 101176. <https://doi.org/10.1016/j.redox.2019.101176>
- Walton, J. N., & Nattrass, F. J. (1954). On the classification, natural history and treatment of the myopathies. *Brain*, 77(2), 169–231. <https://doi.org/10.1093/brain/77.2.169>
- Wang, H., Schänzer, A., Kampschulte, B., Daimagüler, H. S., Logeswaran, T., Schlierbach, H., Petzinger, J., Ehrhardt, H., Hahn, A., & Cirak, S. (2018). A novel SPEG mutation causes non-compaction cardiomyopathy and neuropathy in a floppy infant with centronuclear myopathy. *Acta Neuropathologica Communications*, 6(1), 83. <https://doi.org/10.1186/s40478-018-0589-y>
- Wang, T., Xie, X., Liu, H., Chen, F., Du, J., Wang, X., Jiang, X., Yu, F., & Fan, H. (2019). Pyridine nucleotide-disulphide oxidoreductase domain 2 (PYROXD2): Role in mitochondrial function. *Mitochondrion*, 47, 114–124. <https://doi.org/10.1016/j.mito.2019.05.007>
- Woods, J. D., Khanlou, N., Lee, H., Signer, R., Shieh, P., Chen, J., Herzog, M., Palmer, C., Martinez-Agosto, J., & Nelson, S. F. (2020). Myopathy associated with homozygous PYROXD1 pathogenic variants detected by genome sequencing. *Neuropathology*, 40(3), 302–307. <http://dx.doi.org/10.1111/neup.12641>
- Wu, J. H., & Batist, G. (2013). Glutathione and glutathione analogues; therapeutic potentials. *Biochimica et Biophysica Acta*, 1830(5), 3350–3353. <https://doi.org/10.1016/j.bbagen.2012.11.016>
- Wunderlich, G., Brunn, A., Daimagüler, H. S., Bozoglu, T., Fink, G. R., Lehmann, H. C., Weis, J., & Cirak, S. (2018). Long term history of a congenital core-rod myopathy with compound heterozygous mutations in the Nebulin gene. *Acta Myologica*, 37(2), 121–127.
- Yiş, U., Diniz, G., Hazan, F., Daimagüler, H. S., Baysal, B. T., Baydan, F., Akinci, G., Ünalp, A., Aktan, G., Bayram, E., Hiz, S., Paketçi, C., Okur, D., Özer, E., Danyeli, A. E., Polat, M., Uyanik, G., & Çirak, S. (2018). Childhood onset limb-girdle muscular dystrophies in the Aegean part of Turkey. *Acta Myologica*, 37(3), 210–220.

## SUPPORTING INFORMATION

Additional supporting information may be found online in the Supporting Information section at the end of this article.

**How to cite this article:** Daimagüler H-S, Akpulat U, Özdemir Ö, et al. Clinical and genetic characterization of PYROXD1-related myopathy patients from Turkey. *Am J Med Genet Part A*. 2021;185A:1678–1690. <https://doi.org/10.1002/ajmg.a.62148>